Hindawi
Advances in Materials Science and Engineering
Volume 2017, Article ID 4065434, 9 pages
https://doi.org/10.1155/2017/4065434

Research Article

Effect of Reduction in Thickness and Rolling Conditions on Mechanical Properties and Microstructure of Rolled Mg-8Al-1Zn-1Ca Alloy

Yuta Fukuda,[1] Masafumi Noda,[1] Tomomi Ito,[1] Kazutaka Suzuki,[2] Naobumi Saito,[2] and Yasumasa Chino[2]

[1]*Magnesium Division, Gonda Metal Industry Co. Ltd., Sagamihara, Kanagawa 252-0212, Japan*
[2]*Structural Materials Research Institute of Advanced Industrial Science and Technology (AIST), Nagoya, Aichi 463-8560, Japan*

Correspondence should be addressed to Masafumi Noda; mk-noda@s7.dion.ne.jp

Received 8 March 2017; Revised 17 May 2017; Accepted 31 May 2017; Published 5 July 2017

Academic Editor: Jörg M. K. Wiezorek

A cast Mg-8Al-1Zn-1Ca magnesium alloy was multipass hot rolled at different sample and roll temperatures. The effect of the rolling conditions and reduction in thickness on the microstructure and mechanical properties was investigated. The optimal combination of the ultimate tensile strength, 351 MPa, yield strength, 304 MPa, and ductility, 12.2%, was obtained with the 3 mm thick Mg-8Al-1Zn-1Ca rolled sheet, which was produced with a roll temperature of 80°C and sample temperature of 430°C. This rolling process resulted in the formation of a bimodal structure in the α-Mg matrix, which consequently led to good ductility and high strength, exclusively by the hot rolling process. The 3 mm thick rolled sheet exhibited fine (mean grain size of 2.7 μm) and coarse grain regions (mean grain size of 13.6 μm) with area fractions of 29% and 71%, respectively. In summary, the balance between the strength and ductility was enhanced by the grain refinement of the α-Mg matrix and by controlling the frequency and orientation of the grains.

1. Introduction

A new approach for limiting environmental impact [1] while increasing the speed of a vehicle, by reducing its weight through the replacement of aluminum alloy with lightweight magnesium alloy, has attracted the attention of many researchers [2]. The main disadvantages of using magnesium alloys in a vehicle relate to their combustibility and unsatisfactory mechanical properties. In addition, there is a need to be able to fabricate high strength sheets with a thickness of 3 mm, which approximates the thickness of the sheets that are currently being used. Sakamoto et al. reported that, by adding calcium to a magnesium alloy, the combustion temperature can be increased by more than 250°C [3]. Improvements in the mechanical properties of the magnesium alloys have been achieved by adding different elements [4, 5], applying texture control during forging [6–8], and grain refinement [9]. In most of these studies, rolling [6–9] was used to form the sheets, using extruded material [5, 10, 11] as the starting material.

By focusing on the rolling conditions of magnesium alloys, Sakai reported that, when an AZ31Mg alloy is processed above the recrystallization temperature, there is no tearing; the critical upset ratio is 30% per pass, and the obtained mean grain size is 6 μm after multipass rolling with reheating [12]. Using twin-rolled cast alloy, AMX1001 (mean grain size (d) = 53 μm; initial plate thickness = 3 mm), Noda et al. performed rolling at a roll temperature of 250°C and a sample temperature of 200°C and obtained an elongation of 8% at a tensile strength of 400 MPa [13]. Using extruded sheets of the AZ61 alloy (d = 19 μm) and AM60 alloy (d = 20 μm) with thicknesses of 2 mm, Huang et al. performed hot rolling to achieve a thickness of 0.8 mm and attained an elongation of 26.1% at a tensile strength of 263 MPa [6]. Kim et al. heated an extruded plate with a thickness of 2 mm to 200°C and rolled it to a thickness of 0.7 mm using

Table 1: Chemical composition (mass%) of the Mg-8Al-1Zn-1Ca alloy.

Al	Ca	Zn	Mn	Cu	Ni	Si	Fe	Mg
7.99	0.959	1.076	0.28	0.0014	0.0004	0.0074	0.0022	bal.

different peripheral roll speeds at a roll temperature of 200°C and obtained an elongation of 9–11% at a tensile strength of 394 MPa [7].

The hot rolling of the magnesium alloys have been performed as described above; the initial grain sizes of the samples were as small as 20–50 μm, and high strength or high ductility was achieved by thinning. In other words, there have been no studies reporting a process for fabricating a rolled sheet with a thickness of 3 mm with high strength and high ductility, starting from a cast material with a coarse structure. In this study, we rolled Mg alloys to a total reduction ratio of 75%. We used various materials and rolling temperatures and investigated the influence of the thick-plate rolling conditions on the strength, ductility, and structure.

2. Experiments

In this study, AM60B metal, Mg-30%Ca metal, pure-metal Zn (99.5%), and pure-metal Al (99.7%) were weighed and dissolved to obtain the target composition of the AZX811 alloy, Mg-8Al-1Zn-1Ca mass%. The materials were heated and melted in a steel crucible under an inert argon atmosphere. Then, 0.2 MPa Ar gas was bubbled for 20 min when the melt temperature reached 680°C. After dissolution in the Ar atmosphere and subsequent stirring, the samples were cast by antigravity suction casting [17] with a cooling rate of 12 K/s. Antigravity suction casting was conducted by sinking the down sprue 300 mm into the melt in a SS400 steel mold (95 mm in width, 15 mm in thickness, and 2 m in length), ensuring that the melt was not exposed to the atmosphere during casting. The chemical compositions of the AZX811 cast material are listed in Table 1. The compositional analysis was performed by X-ray fluorescence (JEOL JSX-1000S). To prepare samples for rolling, the cast material was machined into plates measuring 12 mm (H) × 90 mm (W) × 200 mm (L). A two-stage rolling mill was used for the rolling. The rolling samples were heated to 350°C in an electric furnace and then rolled to a thickness of 3 mm with a rolling reduction of 1 mm/pass. The samples were water-cooled after the rolling process; the heating and holding periods were 1 min in each interpass period. The roll temperature was set to 250°C, and the roll peripheral speed was set to 10 m/min.

For tensile tests, samples were cut to a gauge length of 30 mm, 5 mm in width, and 3 mm in thickness by machining, with the longitudinal direction parallel to the rolling direction. The tensile test was performed at room temperature, with an initial strain rate of 1.1×10^{-3} s^{-1}. The elongation after fracture was measured by a noncontact video extensometer (Instron, Type5565, and AVE2). Samples for microstructure observations were prepared by mechanical grinding, polishing, and subsequent etching. The samples were etched using a solution of picric acid (6 g) in ethanol (100 mL), acetic acid (8 mL), and distilled water (10 mL). The structure was observed by optical microscopy (Keyence VHX-2000) and scanning electron microscopy (SEM, JEOL JCM-6000, and JSM-7100F) at an accelerating voltage of 15 kV. The crystallographic orientation was measured using electron backscatter diffraction (EBSD) after ion-polishing of the cross section, parallel to the rolling direction. In relation to the amount of the intermetallic compounds, the area ratio was calculated using a Sigma Scan Pro 5 image analysis software and the grain size was measured by the linear intercept method. The compound formed on the material was qualitatively analyzed by X-ray diffraction (XRD, Rigaku, Smartlab) using a sample measuring 20 mm × 20 mm.

3. Experimental Results and Discussion

3.1. Structure and Mechanical Properties of the Cast Materials. Table 2 lists the mechanical properties of the cast materials, while Figures 1(a)–1(f) show optical and SEM images. The mean grain sizes of the gravity-cast and antigravity-suction-cast materials are 550 μm and 144 μm, respectively. With the decrease in the grain size of the magnesium, the area ratios of the intermetallic compound became 13% and 9% in the gravity-cast and antigravity-suction-cast materials, respectively, as shown in Figures 1(b) and 1(e). The ultimate tensile strength (UTS) and elongation of the antigravity-suction-cast material are 188 MPa and 2.3%, respectively. A comparison between Figures 1(c) and 1(f) showed that the intermetallic compounds were formed discontinuously along the grain boundary, in the antigravity-suction-cast material. Note that Kleiner et al. used a semisolid cast alloy of AZ origin (Al content = 7–9 wt%) to clarify that the ductility is improved by discontinuous scattering in the magnesium region or along the grain boundary, rather than because of the continuous appearance of the beta phase [16]. Yamamoto et al. reported that the strength and ductility are drastically improved when the size of the α-Mg region is reduced to less than 5 μm in the AX43 alloy fabricated by semisolid injection molding [18]. Although the elongation of the cast AZX811 alloy is as low as 2.3%, compared to the mechanical properties of the as-cast magnesium alloys [14, 17, 19] formed by other methods, as listed in Table 2, it is thought that the degree of elongation decreases and high values of the yield strength (YS) and UTS are achieved because an intermetallic compound is formed when 1 mass% of calcium is added.

3.2. Grain Refinement and Improvement of the Mechanical Properties by Multipass Rolling. Figure 2 shows the relationship between the strength, mean grain size d, and total reduction ratio R, observed by multipass rolling to a plate thickness of 12 to 3 mm at a roll temperature (T_R) of 250°C and a sample temperature (T_S) of 350°C. Because fine grains are formed around the coarse grains at a total reduction ratio of 42% or more, the mean grain sizes for the coarse and fine grain areas are also shown in the figure. When the total reduction ratio is 42%, the YS and UTS are 274 MPa and 300 MPa, and the mean grain size decreases to 23 μm. Even if the total reduction ratio is increased to 75%, the YS and UTS are 289 MPa and 322 MPa, respectively, and the mean

Table 2: Mechanical properties of several Mg cast alloys.

Casting process	Materials	YS (MPa)	UTS (MPa)	Elongation (%)	Ref.
Squeeze casting	AZ91	104	183	4.5	[14]
Rheocasting	AZ91	105	171	3.4	[14]
	AZ71	98	185	4.7	[14]
Thixocasting	AZ80	102	187	3.5	[14]
	AX43	117	130	0.5	[15]
Gravity casting	AZX811	130	167	1.5	This work
Antigravity suction casting	AZX811	167	188	2.3	This work
	AMX1001	122	150	2	[16]

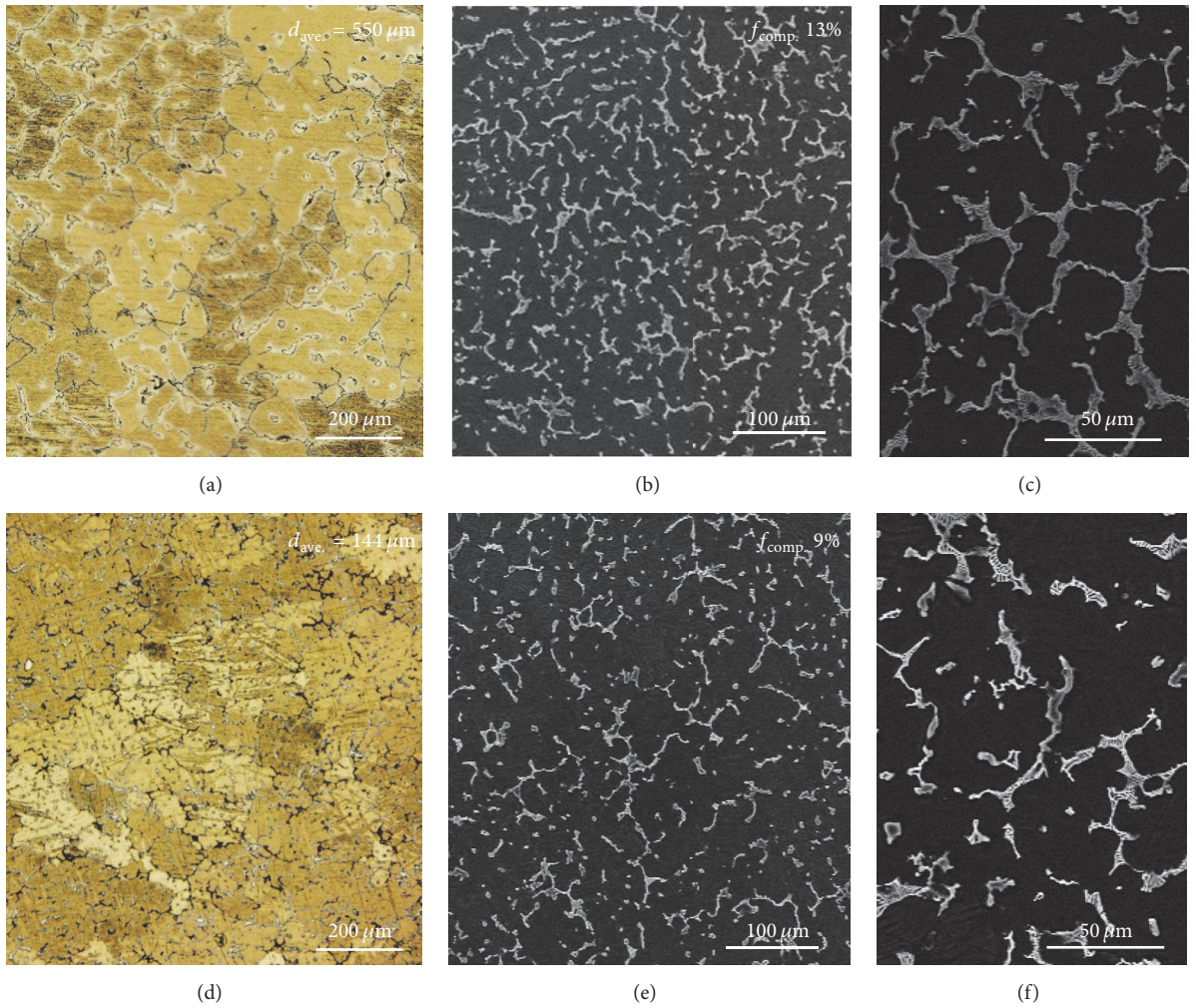

Figure 1: Optical and SEM micrographs of the (a)–(c) gravity-cast and (d)–(f) antigravity-suction-cast alloys. The high-magnification SEM micrographs are shown in (c) and (f).

grain size is 7.6 μm. Figure 3 shows the relationship between YS and elongation for $d^{-1/2}$, as the degree of improvement in strength and the degree of grain refinement are reduced at a total reduction ratio of 42%. The relationship between YS and $d^{-1/2}$ was divided into two linear-gradient (k value) regions. The point of contact between the two straight lines corresponds to R = 42%. There have been many reports addressing the Hall-Petch equation for magnesium alloys, where the value of k is known to depend on the processing temperature [7], grain size [7, 14, 15], sampling direction [8, 15], twin formation [8, 20], and rolling texture [8, 14]. Figure 4 shows the texture variation resulting from multipass rolling. Both the OM structure and the inverse pole figure (IPF) map indicate that, in the multipass rolling of cast materials,

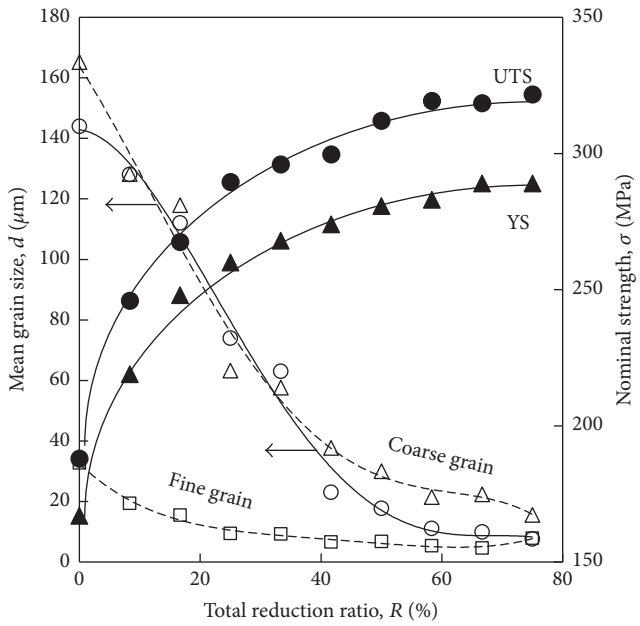

Figure 2: Effect of the total reduction ratio on the strength (yield strength (YS) and ultimate tensile strength (UTS)) and mean grain size of the test specimen. The mean grain sizes of the fine and coarse grain regions are shown.

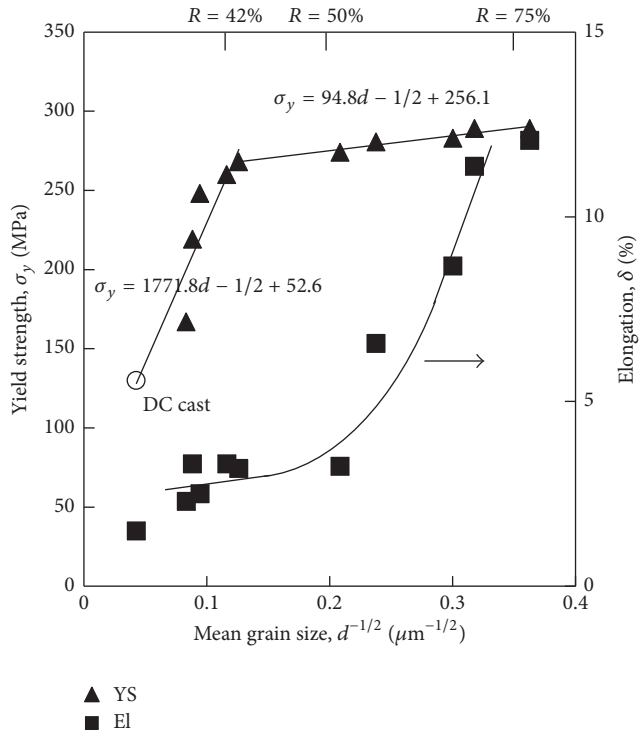

Figure 3: Hall-Petch plots and changes in the elongation as a function of (mean grain size)$^{-1/2}$ under various reduction ratios of the hot-rolled AZX811 alloy. The yield stress of the DC alloy and the total reduction ratio (R) are indicated by the open circle.

twinning deformation occurs inside the coarse grain if the total reduction ratio is less than 42%, thus increasing the difference between the grain boundary directions. The size reduction in the magnesium region because of dynamic recrystallization (DRX) is the dominant factor affecting the strength improvement. On the other hand, if the total reduction ratio exceeds 42%, in general, coarse grains are refined and an intermetallic compound is formed along the boundary of the grains of magnesium, acting as a stress concentration source. Fine grains of less than 7 μm are formed around the grains because of DRX. The IPF map shows that the mean grain size reaches 6.6 μm (area ratio = 44%) at R = 42% in the fine grain area and 7.9 μm (f_{fine} = 75%) at R = 75%. On the other hand, the grain size reached 37.7 μm (f_{coarse} = 56%) in the coarse grain area and 15.6 μm (f_{coarse} = 25%) at R = 75%. Even in a magnesium alloy with added calcium, although the mechanism of the grain refinement acts in the same way as in a AZ series magnesium alloy [6, 7, 21], it is likely that, in the refining of magnesium grains, different factors act in the regions with the total reduction ratio greater than or less than 42%. The intermetallic compound suppresses the grain growth during the heating and holding periods.

Xu et al. showed that the size of the areas around the grain boundary decreased because of the fine dispersion of the beta phase by DRX [22]. del Valle et al. reported that, within the grains, shear deformation and the introduction of twins generate sites of DRX [21]. Although intermetallic compounds were not identified in this study, the optical images shown in Figure 4, the twinning microstructures in the IPF map, and the fine grain region within the magnesium region are consistent with these reports. Jain et al. concluded that the mean grain size has no significant influence on the k value, based on their investigation of the Hall-Petch equation using an extruded AZ31 alloy, for which d = 13–140 μm [15]. However, the influence of the mean grain size cannot be disregarded, because in case of a cast material such as AZX811 alloy, an intermetallic compound exists around the dendrite; the magnesium regions become small as the total reduction ratio increases, and the intermetallic compound aligns parallel to the rolling direction.

3.3. Influence of the Rolling Temperature on the Structure and Mechanical Properties. Figure 2 suggests that the rate of strength improvement decreases as the difference in the mean grain size between the coarse and fine grains of the magnesium decreases with an increase in the total reduction ratio. Therefore, in order to fabricate a sheet thickness of 3 mm, a sheet thickness of 6 mm was used as a starting material for finish rolling and the influence of the rolling conditions shown in Table 3 on the structure and mechanical properties was investigated. Table 3 shows the mechanical properties of sheet thickness of 6 mm. Figure 5 summarizes YS, UTS, and the elongation for each rolling condition. Upon comparing cases 1 and 2, it was found that the UTS does not change at T_R of 250°C, while the elongation increases from 9.5 to 17.9% as a result of increasing T_S. A similar tendency is also observed at T_R = 80°C, and a UTS of 351 MPa and an elongation of 12.2% were obtained in case 4 (T_S = 430°C). When the results were compared to those obtained for the multipass rolling discussed in Section 3.2, in case 4 and in the region

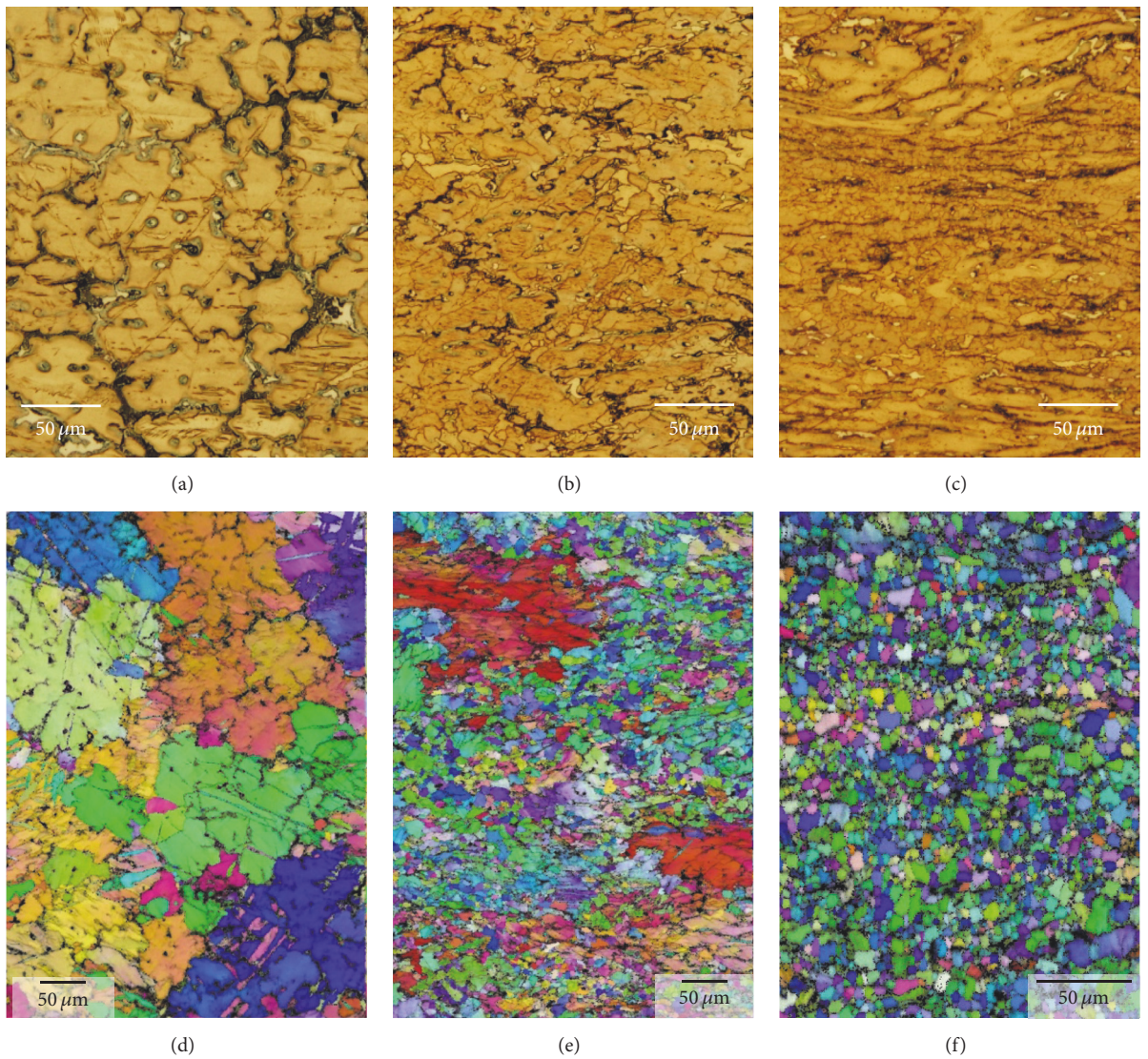

Figure 4: Optical micrographs and inverse pole figure maps of the AZX811 hot-rolled alloy. Total reduction ratios are as follows: (a), (d) 8.3%; (b), (e) 42%; and (c), (f) 75%.

Table 3: Variation in the rolling conditions for samples 6–3 mm in thickness. The mechanical properties and mean grain size of the 6 mm thick alloy are provided.

Case	Roll temp. (°C)	Sample temp. (°C)	Rolling speed (m/min)	t = 6 mm sample properties
The multipass rolling process	250	350	10	d = 17.7 μm YS 281 MPa UTS 312 MPa El 6.6%
1	250	250		
2	250	430		
3	80	250		
4	80	430		

of R = 42–75%, the UTS increased from 22 MPa to 59 MPa in the multipass rolling, as a result of controlling T_R and T_S during the rolling.

For each rolling condition, Figure 6 shows the relationship between the area ratio (f) of the fine grain region, YS, UTS, and elongation, assuming that the plate is rolled to a thickness of 3 mm. The YS and UTS values increased while the elongation decreased from 18 to 2% as the area ratio of the fine grain area increased. Therefore, to compare the internal texture of the rolling materials between case 3, which does not show elongation because of the high mechanical strength, and case 4, in which the mechanical strength and elongation are balanced, Figures 7(a) and 7(b) show the IPF map and the distribution of the grain sizes.

The mean fine grain size and the area ratio are 2.7 μm (f_{fine} = 29%) and 13.6 μm (f_{coarse} = 71%) in case 4 and 2.9 μm (f_{fine} = 65%) and 9.7 μm (f_{coarse} = 35%) in case 3. In case 3, the area ratio of the fine grain area is 65%, but the IPF map shows residual shear deformation caused by the rolling. While both materials showed equivalent image-quality (IQ) levels, a residual processing strain was observed in case 3,

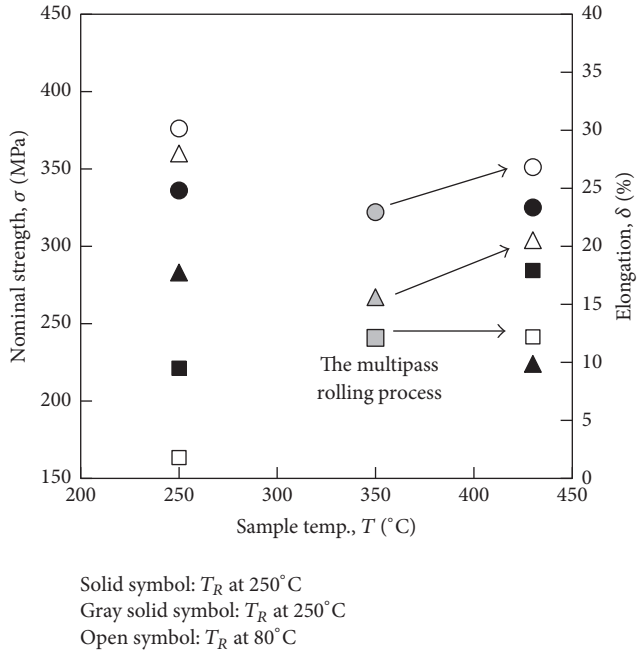

Figure 5: Relationship between the sample temperature and the mechanical properties of case 1 to case 4 and the multipass rolling process result (Section 3.2). The circle, triangle, and square symbols represent UTS, YS, and El, respectively.

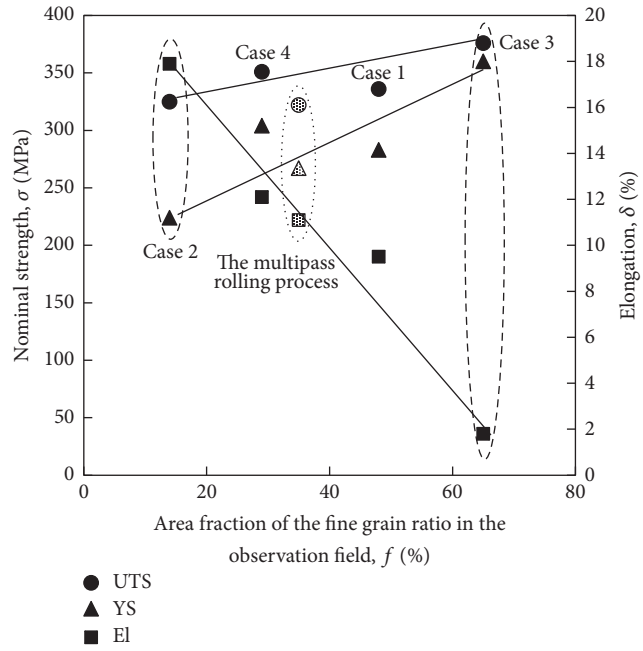

Figure 6: Relationship between the area fraction of the fine grain ratio in the observation field and the mechanical properties under rolling conditions of case 1 to case 4 and the results of the multipass rolling process (Section 3.2). The circle, triangle, and square symbols represent UTS, YS, and El, respectively.

where the black areas with a confidence index (CI) level of less than 0.1 remain. On the other hand, the grain size difference between the areas of the fine and coarse grains in case 4 is 1.6 times greater than that in case 3, and the structure indicates that coarse grains surround the fine grains. The grain size distribution shows that, in case 3, the first peak appears at a mean grain size of 1.3 μm; however, the second peak does not appear subsequently. In case 4, the first peak appears at a mean grain size of 1.3 μm and the second peak appears at a mean grain size of 10–13 μm. Subsequently (up to $d = 30$ μm), the area ratio decreases slowly.

Kato et al. reported that, for homogeneous materials, the strength and ductility can be improved by the presence of connecting fine grains (0.32 μm) around the coarse grains (29.2 μm), although this was only reported for pristine copper [23]. Park and Yanagimoto reported that a warm or hot compression test of 0.2% carbon steel with a bimodal structure, which shows two peaks in the grain distribution, reveals balanced strength and ductility characteristics [24]. The characteristics of the internal structure of the material hot rolled at T_R = 80°C and T_S = 430°C are in agreement with those in the reports discussed above. In other words, to improve both the strength and elongation of the AZX811 alloy exclusively by rolling, it is important for the structure to show a bimodal distribution.

3.4. Rolling Feasibility and Macrorolling Ability. It is well-known that an edge crack develops actively in high strength Mg alloy during the hot rolling process. In this study, for the AZX811 alloy with 1 mass% of added Ca, cracks are likely to occur through the formation of Al-Ca compounds [25]. Figure 8 presents the appearance of the AZX811 rolled sheet at each roll temperature (T_R), sample temperature (T_S), and sheet thickness. For the sheet thickness of 6 mm, edge cracks could not be observed on the rolled sheet. We investigated the edge cracks and the total crack length for rolled sheet thicknesses of 5 to 3 mm, as shown in Figure 8. At the T_S of 250°C, large edge cracks propagated at the T_R of 80°C (case 3) and 250°C (case 1). On the other hand, as T_S was increased to 430°C, the number and length of the edge cracks decreased regardless of the T_R (case 2 and case 4), indicating that the AZX811 alloy has a good roll-ability. In case 2 and case 4, only minor edge cracks were observed on the rolled sheet. By increasing T_R from 80°C to 250°C, the sheets were produced without any obvious edge cracks for each sheet thickness.

The number of edge cracks and the total crack length were measured along the area of 100 mm length, in each sheet thickness [26]. The result is depicted in Figure 9. The number of edge cracks increased with decreasing sheet thickness for each rolling condition. When rolling is performed at a sample temperature of 250°C (case 3), the total crack length and the edge cracks reach 200 mm and 20 pieces, respectively. On the other hand, when rolling was performed at a T_S of 430°C (case 2 and case 4), the number of edge cracks increased with decreasing sheet thickness, but the total crack length did not indicate significant propagation of the cracks. In the rolling process of the AZX811 alloy, it was necessary to set T_S to a high enough temperature to produce a rolled sheet with high strength and elongation and less edge cracks.

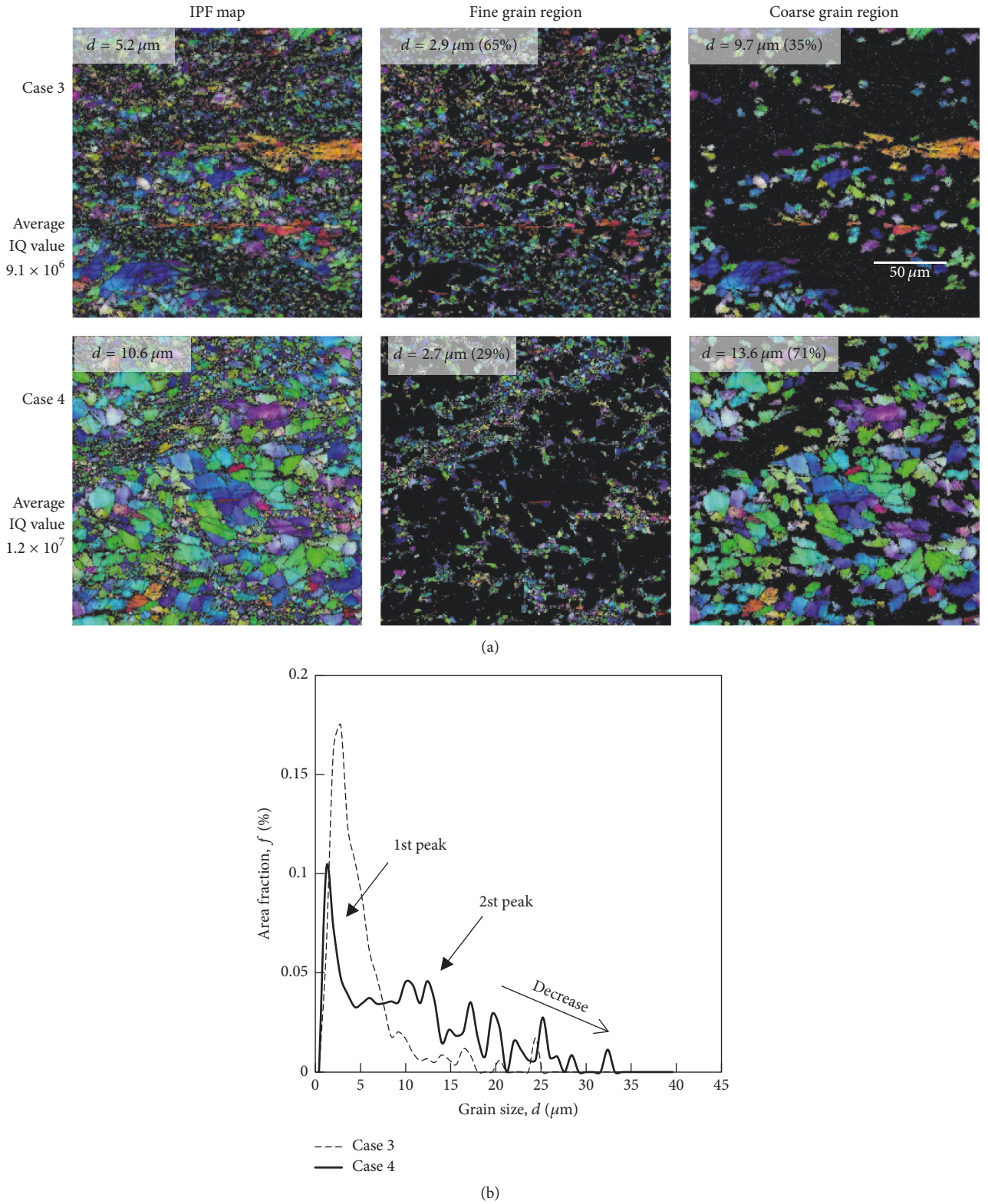

Figure 7: (a) Inverse pole figure maps of the 3 mm thick rolled sample and (b) the grain size distribution diagram. The grain size and area fraction are shown in the IPF maps.

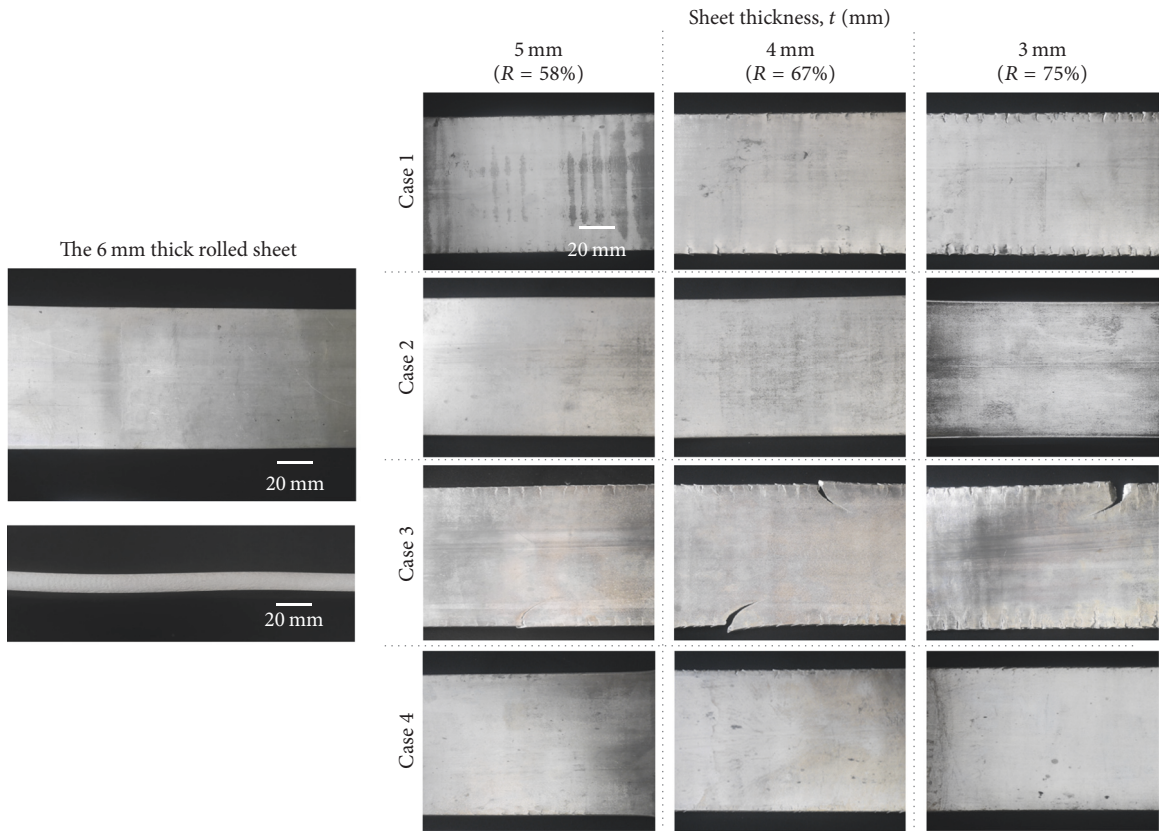

Figure 8: The appearance of the AZX811 rolled sheet at each rolling temperature, sample temperature, and sheet thickness.

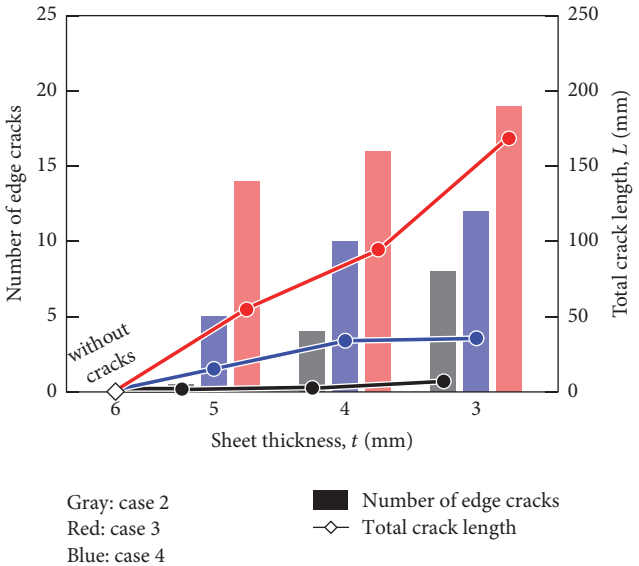

Figure 9: The statistical data on the edge cracks of the rolled sheet at each rolling temperature, sample temperature, and sheet thickness.

4. Conclusion

The influence of the rolling rate, temperature, and intermediate heat treatment was investigated for the fabrication of metal plates with high strength and high ductility using incombustible cast AZX811 alloy as the starting material. In the rolling of cast materials, an improvement in the intensity of the materials was found to depend on the fineness of the magnesium grains up to 42% of the total reduction ratio. On the other hand, at 42% or more of the total reduction ratio, the linear gradient of the Hall-Petch equation changed partially because of the mechanism of grain refining, as affected by the intermetallic compound. Both the strength and ductility are improved by the formation of a bimodal structure, and the material with a plate thickness of 3 mm showed the greatest tensile strength at 351 MPa and an elongation of 12.2%.

Conflicts of Interest

The authors declare that they have no conflicts of interest.

Acknowledgments

This paper is based on results obtained from the Future Pioneering Program (Innovative Structural Materials Project) commissioned by the New Energy and Industrial Technology Development Organization (NEDO).

References

[1] A. A. Luo, "Magnesium: Current and potential automotive applications," *The Minerals, Metals & Materials Society*, vol. 54, pp. 42–48, 2002.

[2] H. Mori, K. Fujino, K. Kurita et al., "Application of the flame-retardant magnesium alloy to high speed rail vehicles," *Materia Japan*, vol. 52, no. 10, pp. 484–490, 2013.

[3] M. Sakamoto, S. Akiyama, T. Hagio, and K. Ogi, "Control of oxidation surface film and suppression of ignition of molten Mg-Ca Alloy by Ca addition," *Journal of Japan Foundry Engineering Society*, vol. 69, pp. 227–233, 1997.

[4] Y. Kawamura and M. Yamasaki, "Formation and mechanical properties of Mg97Zn1RE 2 alloys with long-period stacking ordered structure," *Materials Transactions*, vol. 48, no. 11, pp. 2986–2992, 2007.

[5] S. W. Xu, K. Oh-Ishi, S. Kamado, F. Uchida, T. Homma, and K. Hono, "High-strength extruded Mg-Al-Ca-Mn alloy," *Scripta Materialia*, vol. 65, no. 3, pp. 269–272, 2011.

[6] X. Huang, K. Suzuki, Y. Chino, and M. Mabuchi, "Texture and stretch formability of AZ61 and AM60 magnesium alloy sheets processed by higherature rolling," *Journal of Alloys and Compounds*, vol. 632, pp. 94–102, 2015.

[7] W. J. Kim, J. D. Park, and W. Y. Kim, "Effect of differential speed rolling on microstructure and mechanical properties of an AZ91 magnesium alloy," *Journal of Alloys and Compounds*, vol. 460, no. 1-2, pp. 289–293, 2008.

[8] W. Z. Chen, X. Wang, M. N. Kyalo, E. D. Wang, and Z. Y. Liu, "Yield strength behavior for rolled magnesium alloy sheets with texture variation," *Materials Science and Engineering A*, vol. 580, pp. 77–82, 2013.

[9] J. A. del Valle and O. A. Ruano, "Effect of annealing treatments on the anisotropy of a magnesium alloy sheet processed by severe rolling," *Materials Letters*, vol. 63, no. 17, pp. 1551–1554, 2009.

[10] S. H. Park, S.-H. Kim, Y. M. Kim, and B. S. You, "Improving mechanical properties of extruded Mg-Al alloy with a bimodal grain structure through alloying addition," *Journal of Alloys and Compounds*, vol. 646, Article ID 34372, pp. 932–936, 2015.

[11] M. Hirano, M. Yamasaki, K. Hagihara, K. Higashida, and Y. Kawamura, "Effect of extrusion parameters on mechanical properties of $Mg_{97}Zn_1y_2$ alloys at room and elevated temperatures," *Materials Transactions*, vol. 51, no. 9, pp. 1640–1647, 2010.

[12] T. Sakai, "Microstructure and texture control of magnesium alloy sheets by rolling," *Journal of the Japan Society for Technology of Plasticity*, vol. 50, no. 578, pp. 201–205, 2009.

[13] M. Noda, K. Funami, H. Mori, Y. Gonda, and K. Fujino, "Thermal stability, formability, and mechanical properties of a high-strength rolled flame-resistant magnesium alloy," in *Light Metal Alloys Applications*, A. M. Waldemar, Ed., pp. 125–144, InTech, Rijeka, Croatia, 2014.

[14] W. Yuan, S. K. Panigrahi, J. Q. Su, and R. S. Mishra, "Influence of grain size and texture on Hall-Petch relationship for a magnesium alloy," *Scripta Materialia*, vol. 65, no. 11, pp. 994–997, 2011.

[15] A. Jain, O. Duygulu, D. W. Brown, C. N. Tomé, and S. R. Agnew, "Grain size effects on the tensile properties and deformation mechanisms of a magnesium alloy, AZ31B, sheet," *Materials Science and Engineering A*, vol. 486, no. 1-2, pp. 545–555, 2008.

[16] S. Kleiner, O. Beffort, A. Wahlen, and P. J. Uggowitzer, "Microstructure and mechanical properties of squeeze cast and semi-solid cast Mg-Al alloys," *Journal of Light Metals*, vol. 2, no. 4, pp. 277–280, 2002.

[17] T. Ito, M. Noda, H. Mori, Y. Gonda, Y. Fukuda, and S. Yanagihara, "Effect of antigravity-suction-casting parameters on microstructure and mechanical properties of Mg-10Al-0.2Mn-1Ca cast alloy," *Materials Transactions*, vol. 55, no. 8, pp. 1184–1189, 2014.

[18] Y. Yamamoto, N. Sakate, and K. Sakamoto, "Cast-forge process for Al-Ca series magnesium alloy mold by semi solid injection molding," *Transactions of the Japan Society of Mechanical Engineers, Part A*, vol. 77, no. 780, pp. 1388–1397, 2011.

[19] T. Ito, S. Yanagihara, M. Noda, and H. Mori, "Effect of cast structure and forging conditions on upset forgeability of a flame-resistant magnesium alloys," *Journal of Japan Institute of Light Metals*, vol. 65, no. 12, pp. 611–616, 2015.

[20] Y. N. Wang, C. I. Chang, C. J. Lee, H. K. Lin, and J. C. Huang, "Texture and weak grain size dependence in friction stir processed Mg-Al-Zn alloy," *Scripta Materialia*, vol. 55, no. 7, pp. 637–640, 2006.

[21] J. A. del Valle, M. T. Pérez-Prado, and O. A. Ruano, "Texture evolution during large-strain hot rolling of the Mg AZ61 alloy," *Materials Science and Engineering A*, vol. 355, no. 1-2, pp. 68–78, 2003.

[22] S. W. Xu, N. Matsumoto, S. Kamado, T. Honma, and Y. Kojima, "Dynamic microstructural changes in Mg-9Al-1Zn alloy during hot compression," *Scripta Materialia*, vol. 61, no. 3, pp. 249–252, 2009.

[23] S. Kato, C. Swangrat, O. Yamaguchi, Y. Sudo, D. Orlov, and K. Ameyama, "Microstructure and mechanical properties of harmonic structure designed pure copper," in *Proceedings of the Collected Abstracts of the 2013 Autumn Meeting of the Japan Institute of Metals and Materials*, 2013, J26.

[24] H.-W. Park and J. Yanagimoto, "Formation process and mechanical properties of 0.2% carbon steel with bimodal microstructures subjected to heavy-reduction single-pass hot/warm compression," *Materials Science and Engineering A*, vol. 567, pp. 29–37, 2013.

[25] C. D. Yim, B. S. You, J. S. Lee, and W. C. Kim, "Optimization of hot rolling process of gravity cast AZ31-xCa (x = 0–2.0 mass%) alloys," *Materials Transactions*, vol. 45, no. 10, pp. 3018–3022, 2004.

[26] F. Guo, D. Zhang, X. Yang, L. Jiang, S. Chai, and F. Pan, "Influence of rolling speed on microstructure and mechanical properties of AZ31 Mg alloy rolled by large strain hot rolling," *Materials Science and Engineering A*, vol. 607, pp. 383–389, 2014.